UMT PRESS

Journal of Mathematical Sciences and Informatics
Journal Homepage: https://journal.umt.edu.my/index.php/jmsi
eISSN: 2948-3697
DOI: http://doi.org/10.46754/jmsi.2024.12.003

ANALYTICAL STUDY OF VARIABLE FLUID PROPERTIES AND MAGNETIC FIELD IN THIN-FILM FLOW OVER A STRETCHING STEADY SURFACE

ALI REHMAN AND ZABIDIN SALLEH*

Special Interest Group on Modelling and Data Analytics, Faculty of Computer Science and Mathematics, Universiti Malaysia Terengganu, 21030 Kuala Nerus, Terengganu, Malaysia.

**Corresponding author: zabidin@umt.edu.my*

ARTICLE INFO

Article History:
Received 15 April 2024
Accepted 12 November 2024
Published 15 December 2024

Keywords:
Water based GO-EG nanofluid;
water based GO-W nanofluid;
OHAM;
MHD;
steady stretching surface.

ABSTRACT

This study examines the influence of dynamic viscosity on the steady thin-film flow of water-based nanofluids graphene oxide-ethylene glycol and graphene oxide-water over a stretching surface under the effects of a magnetic field, variable thermal conductivity, and convective boundary condition. The partial differential equations are transformed into nonlinear third order ordinary differential equations using a similarity transformation. The nonlinear equations are solved analytically using the optimal homotopy analysis method. Key velocity and temperature profile parameters are analysed through graphical representations and discussions. The convergence of the solution is validated using the BVPh 2.0 package up to 25 iterations. Additionally, a table summarising the skin friction coefficient and Nusselt number is provided.

2020 Mathematics Subject Classification: 65M25, 76W05

Introduction

Thin-film flow analysis has many uses and applications in engineering, technology, and industrial domains. Thin-film flow exertion has been observed in several settings, from specific processes in human lungs to disruptions in industrial lubricants, yielding a number of outcomes. One of the key areas of thin-fluid flow research is its practical application, which integrates structural mechanics, rheology, and fluid mechanics. Notable applications include its use as a fudge primer, link cable, metal extrusion, exchanges, chemical treatment equipment, drawing of elastic sheets, streaking of objects, steady moulding, and fluidisation of devices. Given these applications, the analysis of fluid films over stretching surfaces is a crucial area of study. Initially, fluid film flows were examined for viscous fluids, and the focus has since expanded to include non-Newtonian liquids.

Sandeep *et al*. [1] analysed thin-film fluid flow using non-Newtonian nanofluid heat transfer. Wang *et al*. [2] illustrated the stretching of an unstable surface by a thin film of fluid. Usha *et al*. [3] examined the formation of thin fluids on an unstable, extended sheet. Liu *et al*. [4] discussed the flow of films under the application of heat on a stretched surface. Aziz *et al*. [5] investigated the potential for internal heat generation in a thin fluid layer passing over an expanding sheet. Tawade *et al*. [6] employed the Newton-Rapson and Runge-Kutta Fehlberg methods to model a thin-film fluid stream with heat transfer in the presence of thermal radiation to organise a nonlinear equation. Anderssona *et al*. [7] discussed heat transfer in a fluid film over an extended sheet. Power laws for fluid flow and liquid film on unstable, extending surfaces have been studied for progressively more complex scenarios [8-11]. Megahe *et al*. [12] explored the effect of slip velocity in the presence

of heat transfer and viscid scattering on a thin Casson liquid stream over an unstable, extending sheet. More recently, Khan *et al*. [13] and Tahir *et al*. [14] studied thin-film nanofluids with novel modifications.

Due to their unique properties, nanofluids are utilised in a wide range of applications, including energy units, medicinal systems, crossover-controlled engines, microelectronics, and, increasingly, in the field of nanotechnology. Previous studies have shown that nanofluids consist of particles smaller than 100 nm. Compared with base fluids such as oil or water, nanofluids exhibit reduced fluid loss of nanoparticles, which is attributed to their enhanced fundamental physical properties, such as heat diffusivity, conductivity, consistency, and convective heat transfer coefficients. A wide range of contemporary processes involve the transfer of thermal energy. In recent years, there has been continuous progress in the development of high-performance thermal systems aimed at enhancing heat exchange. Building on Buongiorno's concept, researchers have investigated nanofluid flow over unstable, expanding sheets [15]. Hayat *et al*. [16] examined Maxwell nanofluids, while Malik *et al*. [17] studied Erying-Powell nanofluids in magnetohydrodynamic (MHD) mixed convective flows. Nadeem *et al*. [18] analysed the movement of Maxwell fluids along a vertically stretching surface in the presence of nanoparticles. Raju *et al*. [19] investigated MHD nano non-Newtonian fluid flow over a cone, focusing on heat and mass transfer in free convection. Rokni *et al*. [20] considered heat exchange in nanofluid streams passing through parallel plates. Nadeem *et al*. [21] numerically studied nanofluid flow over an extending sheet. Shehzad *et al*. [22] explored Jaffrey nanofluid MHD flow under convective boundary conditions.

Sheikholeslami *et al*. [23] investigated nanofluid flow in the presence of a magnetic field during heat transfer. Mahmoodi *et al*. [24] examined the use of heat-exchanging nanofluid flows for cooling purposes. Shah *et al*. [25-27] studied the effects of heat radiation and lobby current with a rotating framework on nanofluid streams. Sheikholeslami's recent theoretical work on nanofluids, involves the examination of various phenomena, applications, assets, and properties through diverse approaches [28-32]. Rehman *et al*. [18] explored Marangoni convection in a water-based carbon nanotube nanofluid over a stretched cylinder. Rehman *et al*. [33] also investigated the viscous dissipation of thin-layer unstable nanofluid flows over a stretching sheet. Balandin *et al*. [34] examined the use of single-layer graphene as a solvent to enhance the thermal efficiency of base fluids. Wei *et al*. [35] demonstrated how graphene oxide's steady diffusion in ethylene glycol improves heat transfer. Gul *et al*. [36] analysed the steady dispersion of graphene nanoparticles and graphene oxide-water (GO-W) nanofluids using a spinning disc model. Gul *et al*. [37] also studied Marangoni convection in nanofluids containing graphene oxide, both in ethylene glycol and water. Other studies [40-50] have explored various geometers and nanofluids, focusing on the impact of different parameters on velocity and temperature profiles.

This study examines the impact of dynamic viscosity on the steady thin-film flow of water-based nanofluids graphene oxide-ethylene glycol (GO-EG) and GO-W under a convective boundary condition, a magnetic field, and varying thermal conductivity over a stretching surface. The nonlinear problem is analytically addressed using the optimal homotopy analysis method (OHAM). Key findings for temperature and velocity profile parameters are presented through plots and discussed. Convergence is achieved within 25 iterations using the BVPh 2.0 tool. Additionally, the Nusselt number and skin friction coefficient are tabulated.

Mathematical Formulation

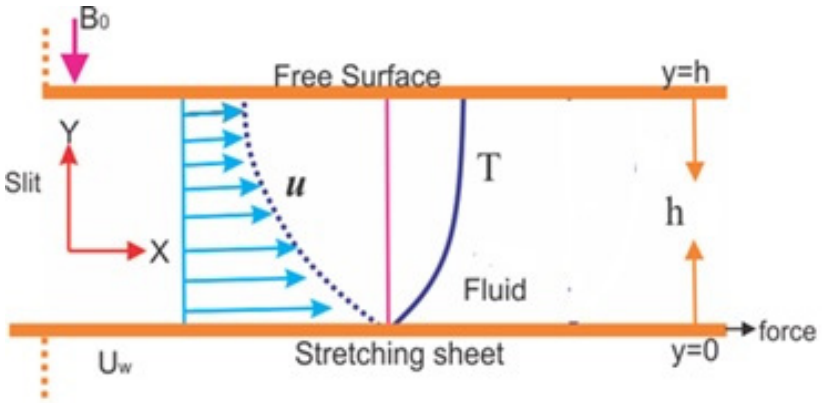

Figure 1: The geometry of the problem

This study examines the time-independent thin-film flow of nanofluids based on GO-W and GO-EG over a stretched surface. The surface exhibits a constant, adjustable velocity $U_w = \frac{bx}{1-\gamma}$ in the x direction, where b and η are positive constants. According to Faraday's law, the flow pattern is influenced by a uniform magnetic field applied in the upward direction perpendicular to the surface. The magnetic field parameter M is defined as $M = \frac{\sigma B_0^2}{\alpha \rho_f}$. The surface temperature distribution $T_w = T_0 - T_r\left(\frac{bx^2}{2\nu}\right)(1-\gamma)^{-\frac{3}{2}}$ varies with the distance x from the slit. The boundary layer equations for continuity, momentum, and heat transfer are derived and expressed as follows [39]:

$$\frac{\partial u}{\partial x} + \frac{\partial v}{\partial v} = 0 \tag{1}$$

$$u\frac{\partial u}{\partial x} + v\frac{\partial u}{\partial y} = \nu\frac{\partial_2 u}{\partial y^2} + \left[\frac{(1-c_\infty)\rho_{nf}\beta f_\infty (T-T_\infty)}{\rho_{nf} f} - \frac{\left(\rho_{nf\,p} - \rho_{nf\,\infty}\right)(c-c_\infty)}{\rho_{nf}} - \frac{\sigma B_0^2 (u-U_\infty)}{\rho_{nf}}\right] g, \tag{2}$$

$$u\frac{\partial T}{\partial x} + v\frac{\partial T}{\partial y} = \alpha\frac{\partial_2 T}{\partial y^2} + \tau\left[\frac{\partial C}{\partial y}\frac{\partial T}{\partial y} + \left(\frac{D_T}{T_\infty}\right)\left(\frac{\partial T}{\partial y}\right)^2\right] + \frac{v}{c_p}\left(\frac{\partial u}{\partial y}\right)^2 + \frac{\sigma B_0^2}{\rho_{nf}\left(c_p\right)_{nf}}\left(u-U_\infty\right)^2 \tag{3}$$

where u and v represent the velocity components along the x-axis and y-axis, respectively. The density of the water-based nanofluid is denoted by ρ_{nf}, while α refers to the dynamic viscosity. The volume fraction of the nanofluid is indicated by C, and U_∞ represents the velocity of the fluid. The electrical conductivity is denoted by σ_{nf}, while τ represents the thermal effect of the heat capacity of nanoparticles and the base liquid. Additionally, T refers to the temperature of the fluid near the wall, and T_∞ denotes the temperature of the fluid at the boundary.

The Brownian motion parameter is denoted by N_b and is defined as $N_b = \frac{\tau D_B C_\infty}{\alpha}$. The thermophoresis parameter is represented by $N_t = \frac{\tau D_T (T_w - T_\infty)}{\alpha T_\infty}$. The Prandtl number is defined as $P_r = \frac{\nu}{\alpha}$. The modified Eckert number is given as $Ec = \frac{U_w}{c_p(T_w - T_\infty)}$. The ratio of the velocity of fluid

at distance to the velocity near the wall is denoted by $A = \frac{U_\infty}{u_b}$. The bioconvection Peclet number is represented as $p_e = \frac{bW_\infty}{D_m}$. The similarity transformation is given by:

$$\eta = \left(\frac{a}{v}\right)^{\frac{1}{2}} y, \psi(x,y) = (av)^{\frac{1}{2}} x f(\eta)$$
$$\theta(\eta) = \frac{T - T_\infty}{T_w - T_\infty} \tag{4}$$

The stream function ψ is defined as:

$$u = \frac{\partial \psi}{\partial y} \text{ and } v = -\frac{\partial \psi}{\partial x} \tag{5}$$

Ordinary differential equations must be derived to transform the partial differential equations. By applying the similarity transformation from Equation (4) to Equations (2) and (3), the following nonlinear ordinary differential equations are obtained:

$$f''' + \frac{1}{(1+\alpha\theta)(1-\phi)^{2.5}}\left(1 - \phi + \phi\left(\frac{\rho_s}{\rho_f}\right)\right) ff'' - (f')^2 - \left(1 - \phi + \phi\left(\frac{(\rho\beta)_s}{(\rho\beta)_f}\right)\right) Mf' = 0 \tag{6}$$

$$\frac{k_{nf}}{k_f}(1+\alpha\theta)\theta'' + \left[\left(1 - \phi + \phi\left(\frac{(\rho c_p)_s}{(\rho c_p)_{nf}}\right)\right)\right][1+\alpha\theta] N_b\theta' + N_t\theta'^2 + \left[\left(1 - \phi + \phi\left(\frac{(\rho c_p)_s}{(\rho c_p)_{nf}}\right)\right)\right][1+\alpha\theta] Ecprf\theta' = 0 \tag{7}$$

with the boundary condition:

$$f(0) = 0, f'(0) = 1 \text{ and } \theta'(0) = 1, \theta(\infty) = 0 \tag{8}$$

The skin friction coefficient and the Nusselt number are defined as:

$$C^*_{fx} = \mathrm{Re}_x^{\frac{1}{2}} C_{fx} = \left(\frac{X}{L}\right)^2 f''(0) \tag{9}$$
$$Nu^*_x = \mathrm{Re}_x^{-\frac{1}{2}} Nu_x = -\theta'(0)$$

Method of Solution

Equations (6) and (7) are solved analytically using OHAM, which is expressed as:

$$L(u(x)) + N(u(x)) + g(x) = 0, B(u(x)) \tag{10}$$

where L is the linear operator, x is the independent variable, $g(x)$ is the unknown function, N is the nonlinear operator, and $B(u)$ is the boundary operator. By applying this method, a family of equations is derived:

$$H(\phi(x), p) = (1-p)\left[L(\phi(x,p)) + g(x)\right] - H(p)\left[L(\phi(x,p)) + g(x) + N(\phi(x,p))\right] = 0$$
$$B(\phi(x,p)) = 0 \tag{11}$$

where p is the embedding parameter, which lies in the interval [0,1], $H(p)$ is a nonzero auxiliary

function for $p \neq 0$, $H(0) = 0$, and $\phi(x,p)$ is an unknown function. Using the initial guessed values and auxiliary linear operators, as given in Equations (8) and (9), the following expressions are obtained:

$$f_0(\eta) = \frac{(b-m)}{24}\eta^4 + \frac{c_2\eta^2}{2} - f_0 = 0 \tag{12}$$

$$L_f = \frac{d^4 f}{d\eta^4}, \quad L_\theta = \frac{d^2\theta}{d\eta^2}, \tag{13}$$

with the constant properties given by:

$$L_f\left(C_1 + C_2\eta + C_3\eta^2 + C_4\eta^3\right) = 0 \quad \text{and} \quad L_\theta\left(C_5 + C_6\eta\right) = 0. \tag{14}$$

where C_i $(i = 1,...,6)$ are arbitrary constants included in the general solution.

Equations (7) and (8) represent the average squared residual error, and they can be expressed as:

$$\varepsilon_m^f = \frac{1}{n+1}\sum_{j=1}^{n}\left[\kappa_f\left(\sum_{j=1}^{n} f(\eta)_{\eta=j\delta\eta}\right)\right], \tag{15}$$

$$\varepsilon_m^\theta = \frac{1}{n+1}\sum_{j=1}^{n}\left[\kappa_\theta\left(\sum_{j=1}^{n} f(\eta)_{\eta=j\delta\eta}, \sum_{j=1}^{n}\theta(\eta)_{\eta=j\delta\eta}\right)\right], \tag{16}$$

$$\varepsilon_m^t = \varepsilon_m^f + \varepsilon_m^\theta. \tag{17}$$

Results and Discussion

This section examines the effects of various parameters, which are the magnetic parameter M, Brownian motion parameter N_b, thermophoresis parameter N_t, dynamic viscosity α, Prandtl number P_r, and Eckert number Ec, on the distribution of velocity and temperature. The numerical results in Tables 1 and 2 illustrate the influence of these model parameters on the skin friction coefficient and Nusselt number for both GO-EG and GO-W. Table 1 shows the impact of various parameters on the local skin friction coefficient, indicating that the skin friction coefficient decreases for both GO-EG and GO-W as the squeezed flow index and magnetic field increase. Table 2 demonstrates that as the Prandtl and Weissenberg numbers increase, the Nusselt number coefficient decreases for both GO-EG and GO-W.

Table 1: Comparison of the skin friction coefficients of the two nanofluids when Pr = 5.6, α = 0.1, $N_t = 1$

N_b	M	$GO-EG$ C^*_{fx}	$GO-W$ C^*_{fx}
0.7	0.5	0.339705	0.29471
0.8		0.32164	0.279547
0.9		0.31147	0.27264
	0.6	0.3100877	0.26994
	0.7	0.30608	0.23724
		0.298432	0.2246
		0.25818	0.21641

Table 2: Comparison of the Nusselt number ($\mathrm{Re}_x^{-1/2} Nu_x$) for the two nanofluids when $N_t = 1, M = 10, Ec = 5, \alpha = 0.9$

Pr	N_t	$GO-EG$ $\boldsymbol{Nu^*_x}$	$GO-W$ $\boldsymbol{Nu^*_x}$
5	0.3	0.41231	0.39077
7		0.39341	0.38237
9		0.37451	0.37397
	0.5	0.35614	0.35647
	0.7	0.33776	0.34897
		0.32795	0.33121
		0.31021	0.31346

The convergence for both GO-EG and GO-W nanofluids has been achieved up to the 25th iteration, as shown in Tables 3 and 4. They demonstrate how decreasing the order of residual error and achieving strong convergence can be accomplished by increasing the number of iterations. Figure 2 illustrates the effect of the magnetic parameter on the velocity profile. The relationship between velocity and dynamic viscosity is inversely proportional to the magnetic parameter. As the magnetic field increases, resistance forces are generated, partially hindering the fluid's motion, resulting in a decrease in the velocity profile.

Table 3: The convergence of the method for GO-W nanofluid when $\mathrm{Pr} = 9, \mathrm{M} = 10, N_b = 0.5, \alpha = 0.1, Ec = 3$

m	$\varepsilon_m^f\ GO-W$	$\varepsilon_m^\theta GO-W$
5	7.55438 x 10^{-1}	3.86775 x 10^{-1}
10	4.69094 x 10^{-3}	6.48738 x 10^{-2}
15	3.209443 x 10^{-7}	5.07298 x 10^{-4}
20	5.37298 x 10^{-9}	1.54131 x 10^{-5}
25	9.33787 x 10^{-11}	9.94423 x 10^{-6}

Table 4: The convergence of the method for GO-EG when $\mathrm{Pr} = 5, \mathrm{M} = 7, N_t = 0.3, N_b = 0.9, \alpha = 0.5, Ec = 8$

m	$\varepsilon_m^f\ GO-W$	$\varepsilon_m^\theta GO-W$
5	1.18991 x 10^{-1}	7.88574 x 10^{-1}
10	5.47666 x 10^{-2}	5.0759 x 10^{-3}
15	4.53983 x 10^{-3}	3.0759 x 10^{-5}
20	7.4616 x 10^{-4}	6.55721 x 10^{-7}
25	7.19521 x 10^{-5}	8.226632 x 10^{-9}

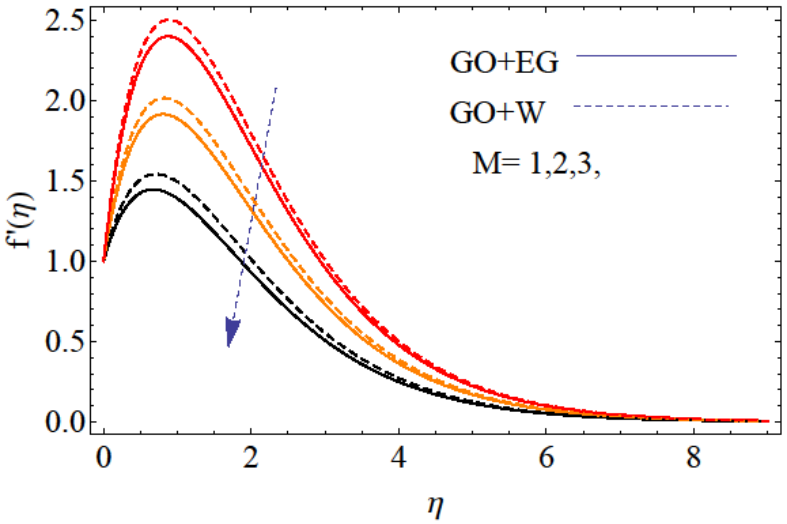

Figure 2: The effect of the magnetic field on the velocity profile

Figure 3 shows the effect of dynamic viscosity on the velocity profile. The relationship between velocity and dynamic viscosity is inverse. As dynamic viscosity increases, the velocity decreases due to the increased dynamic viscosity, making the fluid more viscous and reducing particle movement. Figure 4 illustrates the effect of nanoparticles volume friction on the nanofluid velocity field. The relationship between velocity and nanoparticle volume friction is also inversely. As the nanoparticles volume friction increases, the velocity profile decreases.

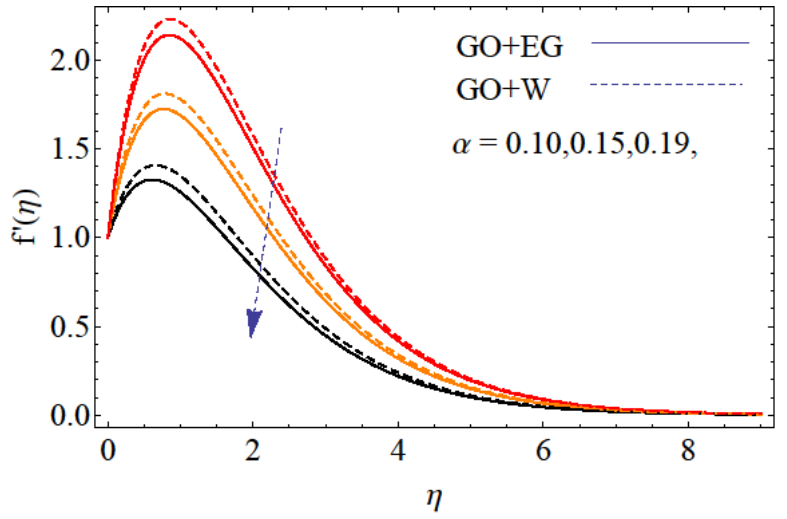

Figure 3: Effect of dynamic viscosity on velocity profile

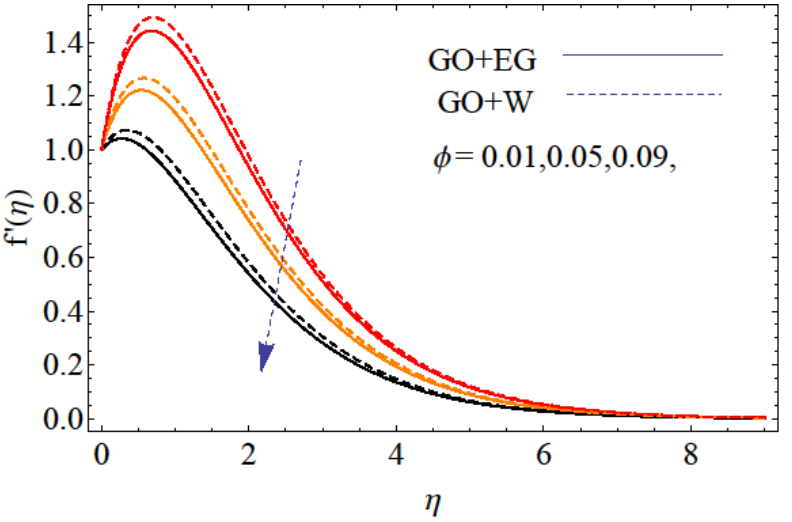

Figure 4: Effect of nanoparticle volume friction on the velocity profile

Figure 5 shows the effect of the Eckert number on the nanofluid temperature field. The relationship between the temperature field and Eckert number is direct, with the temperature profile increasing as the Eckert number rises. Figure 6 illustrates the impact of the Prandtl number on the temperature field $\theta(\eta)$. The relationship between the temperature field and Prandtl number Pr is inverse; as the Prandtl number increases, the temperature profile decreases, as shown in Figure 7. Figure 8 demonstrates the effect of the thermophoresis parameter on the temperature profile. The relationship between the thermophoresis parameter and temperature is direct; increasing the thermophoresis parameter leads to an increase in the temperature profile.

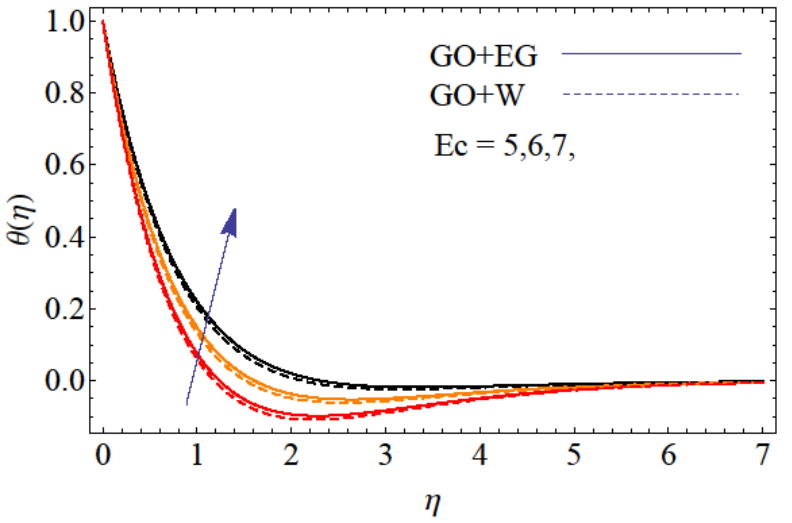

Figure 5: The effect of the Eckert number on the temperature profile

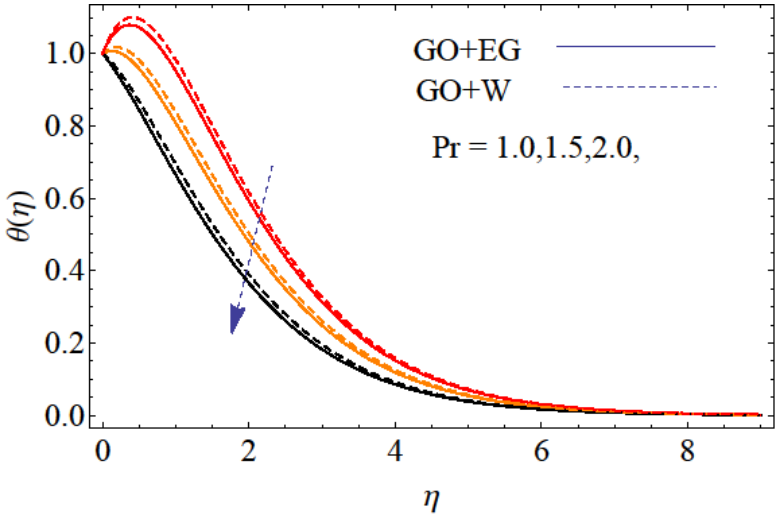

Figure 6: The effect of the Prandtl number on the temperature profile

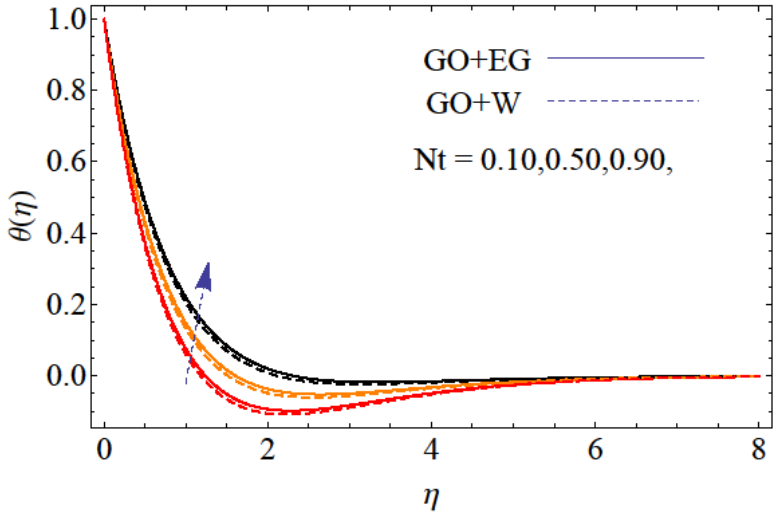

Figure 7: The effect of the thermophoresis parameter on the temperature profile

Conclusions

This study investigates the effect of dynamic viscosity on the steady thin-film flow of water-based nanofluids GO-EG and GO-W in the presence of a magnetic field, varying thermal conductivity, and a convective boundary condition over a stretching surface. Using the similarity transformation, nonlinear third-order ordinary differential equations were derived from the partial differential equations. The nonlinear problem was solved analytically using OHAM. The effects of key parameters on the velocity and temperature profiles were plotted and discussed. Convergence is achieved up to 25 iterations using the BVPh 2.0 package. Tables are provided to present the Nusselt number and skin friction coefficients. The results are as follows:

- Increasing magnetic field decreases the velocity field;
- Increasing dynamic viscosity reduces the velocity profile;
- Increasing the Prandtl number decreases the temperature profile;
- Increasing the Eckert number increases the temperature field;
- Increasing the thermophoresis parameter, increases the velocity profile; and,
- Increasing the nanoparticle volume friction decreases the velocity profile.

Nomenclature

Surface constant	U_w
Velocity of fluid	U_∞
Density of the nanofluids	ρ_{nf}
Electrical conductivity	σ_{nf}
Dynamic viscosity	α
Temperature of fluid near the wall	T
Temperature distribution	T_w
Temperature of fluid near boundary	T_∞
Magnetic field	M
Nusselt number	Nu_x^*
Prandtl number	P_r
Bio convection Peclet number	p_e
Volume fraction of nanofluid	C
Effect of heat capability of nanoparticles and base liquid	τ
Brownian motion parameter	N_b
Thermophoresis parameter/Weissenberg number	N_t
Eckert number	Ec
Skin friction	C_{fx}^*
Velocity components	(u,v)

Acknowledgements

The authors gratefully acknowledge the Research Management Office, Universiti Malaysia Terengganu, for providing partial support for this study. The authors also wish to thanks the reviewers for their careful reading of the paper and useful remarks.

Conflict of Interest Statement

The authors declare that they have no conflict of interest. The funders had no role in the design of the study; in the collection, analyses, or interpretation of data; in the writing of the manuscript, or in the decision to publish the results.

References

[1] Sandeep, N., & Malvandi, A. (2016). Enhanced heat transfer in liquid thin film flow of non-Newtonian nanofluids embedded with graphene nanoparticles. *Advanced Powder Technology*, *27*(6), 2448-2456. https://doi.org/10.1016/j.apt.2016.08.023

[2] Wang, C. Y. (1990). Liquid film on an unsteady stretching surface. *Quarterly of Applied Mathematics*, *48*(4), 601-610. http://www.jstor.org/stable/43637666

[3] Usha, R., & Sridharan, R. (1993). On the motion of a liquid film on an unsteady stretching surface. *Open Journal of Fluid Dynamics*, *150*(1993), 43-48.

[4] Liu, I., & Andersson, H. I. (2007). Heat transfer in a liquid film on an unsteady stretching sheet. *Journal of Thermal Sciences*, *47*(6), 766-772.

[5] Aziz, R.C., Hashim, I. & Alomari, A.K. (2011). Thin film flow and heat transfer on an unsteady stretching sheet with internal heating, *Meccanica*, *46*, 349-357.

[6] Tawade, J., Abel, M. S., Metri, P. G., & Koti, A. (2016). Thin film flow and heat transfer over an unsteady stretching sheet with thermal radiation, internal heating in presence of external magnetic field. *International Journal Advances in Applied Mathematics and Mechanics*, *3*(4), 29-40. http://www.ijaamm.com/uploads/2/1/4/8/21481830/v3n4p5_29-40.pdf

[7] Andersson, H. I., Aarseth, J. B., & Dandapat, B. S. (2000). Heat transfer in a liquid film on an unsteady stretching surface. *International Journal of Heat and Mass Transfer*, *43*(1), 69-74. https://doi.org/10.1016/s0017-9310(99)00123-4

[8] Chen, C. H. (2003). Heat transfer in a power-law fluid film over an unsteady stretching sheet, *International Journal of Heat and Mass Transfer*, *39*(8), 791-796. https://doi.org/10.1007/s00231-002-0363-2

[9] Chen, C. H. (2006). Effect of viscous dissipation on heat transfer in a non-Newtonian liquid film over an unsteady stretching sheet. *Journal of Non-Newtonian Fluid Mechanics*, *135*(2-3), 128-135. https://doi.org/10.1016/j.jnnfm.2006.01.009

[10] Wang, C., & Pop, I. (2006). Analysis of the flow of a power-law fluid film on an unsteady stretching surface by means of homotopy analysis method, *Journal of Non-Newtonian Fluid Mechanics*, *138*(3) (2006), 161-172. https://doi.org/10.1016/j.jnnfm.2006.05.011

[11] Abdelmotalib, H. M., Youssef, M. A., Hassan, A. A., Youn, S. B., & Im, I. (2015). Heat transfer process in gas–solid fluidized bed combustors. *International Journal of Heat and Mass Transfer*, *89*, 567-575. https://doi.org/10.1016/j.ijheatmasstransfer.2015.05.085

[12] Megahed, A. M. (2015). Effect of slip velocity on casson thin film flow and heat transfer due to unsteady stretching sheet in presence of variable heat flux and viscous dissipation. *Applied Mathematics and Mechanics*, *36*(10), 1273-1284. https://doi.org/10.1007/s10483-015-1983-9

[13] Khan, N. S., Gul, T., Islam, S., Khan, A., & Shah, Z. (2017). Brownian motion and thermophoresis effects on MHD mixed convective thin film second-grade nanofluid flow with Hall effect and heat transfer past a stretching sheet. *Journal of Nanofluids*, *6*(5), 812-829. https://doi.org/10.1166/jon.2017.1383

[14] Tahir, F., Gul, T., Islam, S., Shah, Z., Khan, A., Khan, W., Ali, L., & Muradullah, N. (2017). Flow of a nano-liquid film of Maxwell fluid with thermal radiation and magneto hydrodynamic properties on an unstable stretching sheet, *Journal of Nanofluids*, *6*(6) (2017), 1021-1030. https://doi.org/10.1166/jon.2017.1400

[15] Abolbashari, M. H., Freidoonimehr, N., Nazari, F., & Rashidi, M. M. (2015). Analytical modeling of entropy generation for Cassonnano-fluid flow induced by a stretching surface. *Advanced Powder Technology*, *26*(2), 542-552. https://doi.org/10.1016/j.apt.2015.01.003

[16] Hayat, T., Muhammad, T., Shehzad, S. A., & Alsaedi, A. (2015). Three-dimensional boundary layer flow of Maxwell nanofluid: Mathematical model. *Applied Mathematics and Mechanics*, *36*(6), 747-762. https://doi.org/10.1007/s10483-015-1948-6

[17] Malik, M. Y., Khan, I., Hussain, A., & Salahuddin, T. (2015). Mixed convection flow of MHD Eyring–powell nanofluid over a stretching sheet: A numerical study. *AIP Advances*, *5*(11), 117-118. https://doi.org/10.1063/1.4935639

[18] Nadeem, S., Haq, R. U., & Khan, Z. (2014). Numerical study of MHD boundary layer flow of a Maxwell fluid past a stretching sheet in the presence of nanoparticles, *Journal of the Taiwan Institute of Chemical Engineers*, *45*(11), 121-126. https://doi.org/10.1016/j.jtice.2013.04.006

[19] Raju, C. S. K., Sanjeevi, P., Raju, M. C., Ibrahim, S. M., Lorenzini, G., & Lorenzini, E. (2017). The flow of magnetohydrodynamic Maxwell nanofluid over a cylinder with Cattaneo-Christov heat flux model. *Continuum Mechanics and Thermodynamics*, *29*(6), 1347-1363. https://doi.org/10.1007/s00161-017-0580-z

[20] Rokni, H. B., Alsaad, D. M., & Valipour, P. (2016). Electrohydrodynamic nanofluid flow and heat transfer between two plates. *Journal of Molecular Liquids*, *216*, 583-589. https://doi.org/10.1016/j.molliq.2016.01.073

[21] Nadeem, S., Haq, R. U., & Khan, Z. H. (2014). Numerical solution of non-Newtonian nanofluid flow over a stretching sheet. *Applied Nanoscience*, *4*(5), 625-631. https://doi.org/10.1007/s13204-013-0235-8

[22] Shehzad, S. A., Hayat, T., & Alsaedi, A. (2015). MHD flow of Jeffrey nanofluid with convective boundary conditions. *Journal of the Brazilian Society of Mechanical Sciences and Engineering*, *37*(3), 873-883. https://doi.org/10.1007/s40430-014-0222-3

[23] Sheikholeslami, M., Hatami, M., & Ganji, D. (2014). Nanofluid flow and heat transfer in a rotating system in the presence of a magnetic field. *Journal of Molecular Liquids*, *190*, 112-120. https://doi.org/10.1016/j.molliq.2013.11.002

[24] Mahmoodi, M., & Kandelousi, S. (2016). Kerosene−alumina nanofluid flow and heat transfer for cooling application. *Journal of Central South University*, *23*(4), 983-990. https://doi.org/10.1007/s11771-016-3146-5

[25] Shah, Z., Islam, S., Gul, T., Bonyah, E., & Khan, M. A. (2018). The electrical MHD and Hall current impact on micropolar nanofluid flow between rotating parallel plates. *Results in Physics*, *9*, 1201-1214. https://doi.org/10.1016/j.rinp.2018.01.064

[26] Shah, Z., Gul, T., Islam, S., Khan, M. A., Bonyah, E., Hussain, F., Mukhtar, S., & Ullah, M. (2018b). Three dimensional third grade nanofluid flow in a rotating system between parallel plates with Brownian motion and thermophoresis effects. *Results in Physics*, *10*, 36-45. https://doi.org/10.1016/j.rinp.2018.05.020

[27] Shah, Z., Gul, T., Khan, M. A., Ali, I., & Islam, S. (2017). Effects of hall current on steady three dimensional non-Newtonian nanofluid in a rotating frame with Brownian motion and thermophoresis effects, *Journal of Engineering Technology*, *6*(SP), 280-296.

[28] Sheikholeslami, M., Shamlooei, M., & Moradi, R. (2017). Fe3O4-ethylene glycol nanofluid forced convection inside a porous enclosure in existence of Coulomb force. *Journal of Molecular Liquids*, *249*, 429-437. https://doi.org/10.1016/j.molliq.2017.11.048

[29] Sheikholeslami, M. (2017). Numerical investigation of nanofluid free convection under the influence of electric field in a porous enclosure. *Journal of Molecular Liquids*, *249*, 1212–1221. https://doi.org/10.1016/j.molliq.2017.11.141

[30] Sheikholeslami, M., & Rokni, H. B. (2017). Numerical simulation for impact of Coulomb force on nanofluid heat transfer in a porous enclosure in presence of thermal radiation. *International Journal of Heat and Mass Transfer*, *118*, 823-831. https://doi.org/10.1016/j.ijheatmasstransfer.2017.11.041

[31] Shah, Z., Bonyah, E., Islam, S., Khan, W., & Ishaq, M. (2018). Radiative MHD thin film flow of Williamson fluid over an unsteady permeable stretching sheet. *Heliyon*, *4*(10), 825-830. https://doi.org/10.1016/j.heliyon.2018.e00825

[32] Towers, S., Afzal, S., Bernal, G., Bliss, N., Brown, S., Espinoza, B., Jackson, J., Judson-Garcia, J., Khan, M., Lin, M., Mamada, R., Moreno, V. M., Nazari, F., Okuneye, K., Ross, M. L., Rodriguez, C., Medlock, J., Ebert, D., & Castillo-Chavez, C. (2015). Mass media and the contagion of fear: The case of Ebola in America. *PLOS ONE*, *10*(6), 1-13. https://doi.org/10.1371/journal.pone.0129179

[33] Rehman, A., Salleh, Z., Gul, T., & Zaheer, Z. (2019). The impact of viscous dissipation on the thin film unsteady flow of GO-EG/GO-W nanofluids, *Mathematics*, *7*(7), Article 653. https://doi.org/10.3390/math7070653

[34] Balandin, A. A., Ghosh, S., Bao, W., Calizo, I., Teweldebrhan, D., Miao, F., & Lau, C. N. (2008). Superior thermal conductivity of single-layer graphene. *Nano Letters*, *8*(3), 902-907. https://doi.org/10.1021/nl0731872

[35] Yu, W., Xie, H., & Bao, D. (2010). Enhanced thermal conductivities of nanofluids containing graphene oxide nanosheets. *Nanotechnology*, *21*(5), Article 055705. https://doi.org/10.1088/0957-4484/21/5/055705

[36] Gul, T., & Firdous, K. (2018). The experimental study to examine the stable dispersion of the graphene nanoparticles and to look at the GO-H_2O nanofluid flow between two rotating disks. *Applied Nanoscience*, *8*(7), 1711-1727. https://doi.org/10.1007/s13204-018-0851-4

[37] Gul, T., Noman, W., Sohail, M., & Khan, M. A. (2019) Impact of the Marangoni and thermal radiation convection on the graphene-oxide-water-based and ethylene-glycol-based nanofluids. *Advances in Mechanical Engineering*, *11*(6), 1-9. https://doi.org/10.1177/1687814019856773

[38] Rehman, A., Gul, T., Salleh, Z., Mukhtar, S., Hussain, F., Nisar, K. S., & Kumam, P. (2019). Effect of the marangoni convection in the unsteady thin film spray of CNT nanofluids. *Processes*, *7*(6), Article 392. https://doi.org/10.3390/pr7060392

[39] Khan, D., Kumam, P., Kumam, W., Suttiarporn, P., & Rehman, A. (2023). Relative magnetic field and slipping effect on Casson dusty fluid of two phase fluctuating flow over inclined parallel plate. *South African Journal of Chemical Engineering*, *44*, 135-146. https://doi.org/10.1016/j.sajce.2023.01.010

[40] Rehman, A., Khan, W., Bonyah, E., Karim, S. A. A., Alshehri, A., & Galal, A. M. (2022). Steady three-dimensional MHD mixed convection couple stress flow of hybrid nanofluid with hall and ion slip effect. *Advances in Civil Engineering, 2022*(1), 1-11. https://doi.org/10.1155/2022/9193875

[41] Rehman, A., Alhefthi, R. K., Inc, M., & Jan, R. (2024). Analytical investigation of MgO–CuO\H_2O, hybrid nanofluid MHD stagnation point flow with the influence of viscous dissipation for enhancement of heat transfer ratio. *Modern Physics Letters B*, *38*(15), 1-16. https://doi.org/10.1142/s0217984924501082

[42] Rehman, A., Inc, M., Salah, B., & Hussain, S. (2023). Analytical analysis of silver-water, silver-blood base nanofluid flow over fluctuating disk with the influence of viscous dissipation over fluctuating disk. *Modern Physics Letters B*, *37*(32), Article 2350113. https://doi.org/10.1142/s0217984923501130

[43] Rehman, A., Salleh, Z., & Gul, T. (2019). Influence of dynamics viscosity on the water base graphene oxide–ethylene glycol/graphene oxide–water nanofluid flow over a stretching cylinder. *Journal of Nanofluids*, *8*(8), 1661-1667.

[44] Rehman, A., Salleh, Z., & Gul, T. (2019b). The impact of the magnetic field and viscous dissipation on the thin film unsteady flow of GO-EG/GO-W nanofluids. *Journal of Physics Conference Series*, *1366*(1), 012031. https://doi.org/10.1088/1742-6596/1366/1/012031.

[45] Rehman, A., Salleh, Z., & Gul, T. (2019c). The impact of Marangoni convection, magnetic field and viscous dissipation on the thin film unsteady flow of go-eg/go-w nanofluids over an extending sheet. *JP Journal of Heat and Mass Transfer*, *18*(2), 477-496. https://doi.org/10.17654/hm018020477

[46] Rehman, A., Saeed, A., Salleh, Z., Jan, R., & Kumam, P. (2022). Analytical investigation of the time-dependent stagnation point flow of a CNT nanofluid over a stretching surface. *Nanomaterials*, *12*(7), Article 1108. https://doi.org/10.3390/nano12071108

[47] Rehman, A., Khan, W., Abdelrahman, A., Jan, R., Khan, M. S., & Galal, A. M. (2022). Influence of Marangoni convection, solar radiation, and viscous dissipation on the bioconvection couple stress flow of the hybrid nanofluid over a shrinking surface. *Frontiers in Materials*, *9*, Article 964543. https://doi.org/10.3389/fmats.2022.964543

[48] Srivastava, H. M., Khan, Z., Mohammed, P. O., Al-Sarairah, E., Jawad, M., & Jan, R. (2022). Heat transfer of buoyancy and radiation on the free convection boundary layer MHD flow across a stretchable porous sheet. *Energies*, *16*(1), Article 58. https://doi.org/10.3390/en16010058

[49] Zubair, M., Jawad, M., Bonyah, E., & Jan, R. (2021). MHD analysis of couple stress hybrid nanofluid free stream over a spinning darcy-forchheimer porous disc under the effect of thermal radiation. *Journal of Applied Mathematics*, *2021*(2), 1-18. http://dx.doi.org/10.1155/2021/2522155

[50] Chakraborty, T., Das, K., & Kundu, P. K. (2018). Framing the impact of external magnetic field on bioconvection of a nanofluid flow containing gyrotactic microorganisms with convective boundary conditions. *Alexandria Engineering Journal*, *57*(1), 61-71. https://doi.org/10.1016/j.aej.2016.11.011